Mansoura Engineering Journal

Volume 19 | Issue 1 Article 11

3-1-2020

The Numerical Prediction of the Flow Pattern under a Stationary Hovercraft.

Mohamed El-Kady
Assistant Professor Mechanical Power Engineering Department, Faculty of Engineering, Mansoura University, Mansoura, Egypt.

Follow this and additional works at: https://mej.researchcommons.org/home

Recommended Citation
El-Kady, Mohamed (2020) "The Numerical Prediction of the Flow Pattern under a Stationary Hovercraft.," *Mansoura Engineering Journal*: Vol. 19 : Iss. 1 , Article 11.
Available at: https://doi.org/10.21608/bfemu.2021.163018

This Original Study is brought to you for free and open access by Mansoura Engineering Journal. It has been accepted for inclusion in Mansoura Engineering Journal by an authorized editor of Mansoura Engineering Journal. For more information, please contact mej@mans.edu.eg.

Mansoura Engineering Journal (MEJ). Vol. 19, No. 1, March 1994. M. 76

THE NUMERICAL PREDICTION OF THE FLOW PATTERN UNDER A STATIONARY HOVERCRAFT

M. S. Mohamed

Mechanical Power Engineering Department,
Faculty of Engineering, Mansoura University.

التنبؤ العددى بشكل الانسياب تحت حوامة ثابتة

الخلاصة:

الحوامة (المركبة ذات الوسادة الهوائية) هى مركبة برمائية تستخدم فى نقل الافراد والمعدات فى البر والبحر وعلى الجليد ايضا. لذلك يستخدمها الاسطول البحرى لنقل المعدات الحربية من وسط البحر الى الشاطىء. يقدم هذا البحث طريقة عددية للتنبؤ بشكل الانسياب الناتج تحت حوامة ثابتة باستخدام النموذج الرياضى للانسياب اللادورانى. ثلاثة انماط من الانسياب درست فى هذا البحث باستخدام برنامج حاسب آلى يستعمل جريدة مستطيلة للحل. وهذه الانماط هى: شكل الانسياب فى حالة ثبوت معدل سريان الكتلة وشكل الانسياب فى حالة ثبوت ارتفاع فتحة الخروج وأخيرا شكل الانسياب فى حالة ثبوت الضغط المتوسط أسفل سطح الحوامة. تم ايجاد العلاقة بين قيمة الضغط المتوسط ومعدل سريان الكتلة كما تم ايجاد العلاقة بين معدل سريان الكتلة وارتفاع فتحة الخروج (فى حالة ثبوت قيمة متوسط الضغط أسفل سطح الحوامة). وقد بينت النتائج أن شكل الانسياب يتغير مع تغير ارتفاع فتحة الخروج بينما لا يوجد أى تغير فى شكل الانسياب مع زيادة معدل سريان الكتلة فى حالة ثبوت ارتفاع فتحة الخروج. كما قدمت النتائج شرحا للظاهرة العملية لعدم امكانية طفو الحوامة فوق البحار عالية الامواج.

ABSTRACT:

This paper presents a numerical solution procedure for the prediction of the flow pattern created under a stationary hovercraft using the irrotational flow model. A finite difference computer program using a rectangular grid was employed in this study. Three flow patterns are investigated. These flow patterns are the flow pattern at constant mass flow rate M, flow pattern at constant skirt height Y_{gap} and the flow pattern at constant mean pressure along the underside of the hovercraft floor. It, also, determines the dependence of the pressure distribution on the relative height of the skirt and the mass flow rate. The relation between the mass flow rate and the skirt height, at constant average pressure along the underside of the hovercraft, was also obtained. The results show that the flow pattern changes with the variation the the skirt height, while there is no change in the flow pattern with the increase of the mass flow rate, if the skirt height is kept constant. It also explains the practical limitation of the unability of a hovercraft to operate over very rough seas.

1.INTRODUCTION:

Since the 1950's, the Air Cushion Vehicle ACV or hovercraft, has seen widespread commercial application to the transport of people and vehicles over water, land, and ice. Craft are being designed and built for the Army and Navy to carry military payloads from offshore across the beach. Operations have been, and are being, carried out in support of oil and gas exploration and production. The increasing awareness of damage to marshes and tundra by the cutting of canals, or by wheeled or tracked vehicles might suggest a more widespread application for the ACV. Cutt [1] described some existing craft deployments and discussed the key factors that would enhance or limit the role of the ACV in exploration and production of oil and gas.

During operation overwater, hovercraft have been observed to undergo violent self-excited heave oscillations. The hovercraft overwater heave stability was studied by some investigators [2-5]. They identified two potential sources for oscillations. One is a Kelvin-Helmholtz type flutter of the air water interface directly beneath the skirt caused by high speed leakage airflow. The other is a modulation of leakage air flow by complex standing wave directly beneath the craft and its skirts. Experiments and theory show that the flutter mechanism is most active when a craft is equipped with a segment skirt while the standing wave mechanism can be a problem for craft with jupe or cell skirts.

Abulnaga, B. E. [6] reviewed the concept of air propelled vehicles to travel in deserts. He presented an analysis of trafficability problems in Egyptian deserts, with emphasis on sand surfaces. He derived theoretical equations for the prediction of the acceleration and resistance to motion at constant speed and applied them for the French Army's Aero-Roue and the British Army's hovercraft when they operate over sand.

Eroshin et al [7] determined experimentally the pressure on the surface of a disk entering a compressible fluid at an angle to the free surface. The results obtained can be used for designing the structural elements of hovercrafts, water-displacing vessels and hydrofoils.

This paper is interested with the prediction of the flow

pattern beneath a stationary hovercraft using a finite difference solver. The governing equations were derived and implemented into the computer program. The relation between the mass flow rate, skirts gap height and the average pressure along the underside of the hovercraft floor are presented.

2.NATURE OF THE FLOW:

Hovercraft are amphibious vehicles which float on a cushion of pressurized air contained by a flexible structure known as a skirt. Lift air is typically supplied by one or more fans and it leaks away to atmosphere through a gap beneath the skirt.

The flow configuration examined in this paper is shown in figure (1), which represents an idealization of that created under an Air Cushion Vehicle ACV or a stationary hovercraft.

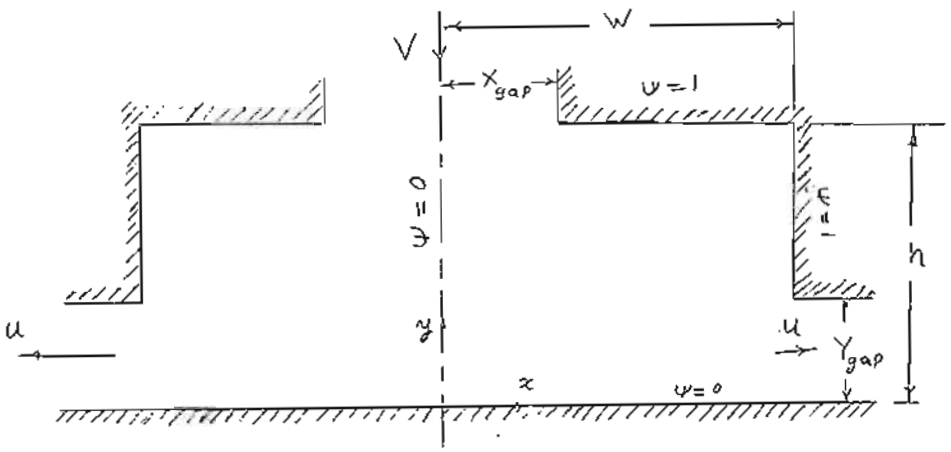

Figure (1) Flow configuration for a stationary hovercraft

paper so that the flow can be treated as two-dimensional. Air and combustion products from the turbines of the hovercraft are admitted through the slot in the roof of the support structure and escape between the lower edge of the skirts and the ground. The ratio w:h is kept here fixed at 5:1 which is fairly representative of practical geometries. The slot in the roof X_{gap} is kept constant and equal to 0.3 w or 1.5 m wide. The height of the skirt gap y_{gap} is a variable and is taken as a ratio of the total height (0.1 h, 0.3 h and 0.5 h) or 0.1 m, 0.3 m, .0.5 m high.

2.1. GOVERNIND EQUATIONS:

In some types of fluid flow the effects of viscous shear are negligible. The neglection of the viscous terms greatly simplifies the aim of solving the equations of motion. For a uniform-density, two dimensional, axisymmetric non-viscous fluid flow; the equations of motion may be written as [8]:

u- momentum equation:

$$\frac{\partial u}{\partial t} + u\frac{\partial u}{\partial x} + v\frac{\partial u}{\partial r} = -\frac{1}{\rho}\frac{\partial \rho}{\partial x} \qquad (1)$$

υ- momentum equation:

$$\frac{\partial \upsilon}{\partial t} + u\frac{\partial \upsilon}{\partial x} + v\frac{\partial \upsilon}{\partial r} = -\frac{1}{\rho}\frac{\partial \rho}{\partial r} \qquad (2)$$

continuity equation:

$$\frac{\partial ru}{\partial x} + \frac{\partial r\upsilon}{\partial r} = 0 \qquad (3)$$

It is obvious, that the equations of motion for plane two dimensional flows can be derived form the above equations by replacing r by 1 and ∂r by ∂y.

The distribution of the two velocity components u, υ as well as the pressure field ρ can be obtained by solving the three above equations simultaneously. It is useful to eliminate the pressure from the two momentum equations by the combination of equations (1) and (2); this is can be done by subtracting the x-derivative of equation (2) from the r-derivative of equation (1). The result may be expressed as:

$$\frac{D\omega}{Dt} \equiv \frac{\partial r\omega}{\partial t} + \frac{\partial}{\partial x}(ru\omega) + \frac{\partial}{\partial r}(rvw) = 0 \quad .....(4)$$

where ω = fluid vorticity $\equiv \dfrac{\partial u}{\partial r} - \dfrac{\partial \upsilon}{\partial x}$ .....(5)

According to equation (4), the vorticity of any fluid element

remains constant. That means if a fluid started from rest, where its vorticity is initially equal to zero everywhere, it will remain zero at all subsequent times.

Inviscid flows, in which the vorticity is everywhere zero, are termed irrotational. For such flows the velocity field is determined from the solution the two partial differential equations given by the continuity equation (3) and the requirement that $\omega = 0$ *i.e.*:

$$\frac{\partial u}{\partial r} - \frac{\partial v}{\partial x} = 0 \qquad \ldots\ldots\ldots\ldots\ldots\ldots (6)$$

Introducing the two dimensional scalar function known as the stream function $\psi\ (x,r)$, defined as (in cylindrical coordinates):

$$\frac{\partial \psi}{\partial r} = \rho r u \qquad \text{and} \qquad \frac{\partial \psi}{\partial x} = \rho r v \qquad \ldots\ldots\ldots (7)$$

in which lines of constant ψ are streamlines. The spacing between the streamlines is inversely proportional to the local velocity as may be seen from the above equation. Moreover, the velocities associated with the $\psi\ (x,r)$ field satisfy from the continuity equation (3). It may be confirmed by substituting equations (7) into equation (3).

Substitution of equations (7) into the irrotationality equation (6) leads to the important result that, In cylindrical coordinates:

$$\frac{\partial}{\partial x}\left\{\frac{1}{r}\frac{\partial \psi}{\partial x}\right\} + \frac{\partial}{\partial r}\left\{\frac{1}{r}\frac{\partial \psi}{\partial r}\right\} = 0 \qquad \ldots\ldots (8)$$

This is what is called the irrotational flow model.

A further important property of irrotational flows may be obtained by multiplying equation (1) by u and adding it to equation (2) multiplied by v. For steady flow the result may be written as

$$\frac{\partial}{\partial x}(ru\rho_t) + \frac{\partial}{\partial r}(rv\rho_t) = 0 \qquad \ldots\ldots\ldots\ldots (9)$$

where p_t denotes for the "total" pressure of the fluid i.e.

$$p_t \equiv p + \rho\,(u^2/2 + v^2/2) = \text{constant} \quad \ldots\ldots\ldots\ldots (10)$$

which is known as "Bernoulli's equation". It states that the total pressure is constant along any streamline or vortex line [9], therefore, in the present case it is constant everywhere in the fluid.

Comparing these equation (8) with the general form of the heat transfer equation solved by the finite-difference computer program TEACH-C [10], which describes the distribution of the temperature T in a stationary medium of density ρ,

$$\rho\, C_v\, r\, \frac{\partial T}{\partial t} - \frac{\partial}{\partial x}\left\{k\, r\, \frac{\partial T}{\partial x}\right\} - \frac{\partial}{\partial y}\left\{k\, r\, \frac{\partial T}{\partial y}\right\} - rs = 0 \qquad (11)$$

where c_v specific heat, t time, k thermal conductivity and s distributed sources or sinks of energy.

It is obvious that, equation (8) fits within framework of the above equation (11), with ψ replaced by T, $\partial T/\partial t$ and s are both set equal to zero, $\partial r = \partial y$ and k is set equal to $1/r^2$. Therefore irrotational flows can be calculated by the same program.

2.2. BOUNDARY AND INITIAL CONDITIONS:

The symmetry of flow allows the calculations to be limited to the half of the hovercraft cross-section, as illustrated in figure (1). Calculations are performed in the rectangular region bounded by the vertical right-hand wall, the horizontal upper wall, the axis of symmetry in the left-hand side and the ground in the lower side. A uniform vertical velocity v is prescribed across the horizontal plane through the horizontal gap x_{gap}, and a uniform horizontal velocity u is set along the vertical plane through the vertical gap y_{gap}. These specifications lead to the boundary values of the stream function ψ for this domain, indicated in figure (1), using equation (7) and the fact that there is no flow through the walls, the ground or the axis of symmetry.

For the parallel flow at inlet through the roof gap x_{gap}, all the flow is in y-direction and there is no flow through the axis of

symmetry. Therefore, equation (7) takes the form:

$$u = \rho \frac{\partial \psi}{\partial y} = 0 \qquad \text{and} \qquad v = - \rho \frac{\partial \psi}{\partial x}$$

The u velocity component states that the stream function ψ is a constant or function of x, f(x), only while the v velocity component indicates that the stream function equals to $\psi = - vx$. Combining the the two statements together, the total stream function for this part of the flow is

$$\psi_1 = - vx$$

At the axis of symmetry, $x = 0$, so $\psi = 0$ while at the top wall $x = x_{gap} = 1.5$, therefore the stream function will be

$$\psi_1 = -1.5\, v \qquad \ldots\ldots\ldots\ldots (12)$$

For the parallel flow at outlet through the skirt height y_{gap}, all the flow is in x-direction and this is no flow through the ground. Therefore, equation (7) becomes:

$$u = \rho \frac{\partial \psi}{\partial y} \qquad \text{and} \qquad v = - \rho \frac{\partial \psi}{\partial x} = 0$$

Employing the same procedure, mentioned above, the total stream function for part of flow is

$$\psi_2 = u\, y \qquad \ldots\ldots\ldots\ldots\ldots (13)$$

At the ground level, $y = 0$, the stream function will be $\psi = 0$ while at the right-hand side wall it takes the form $\psi = u\ y_{gap}$. The skirt height y_{gap} changes form one case to another so the the stream function ψ depends on the values of the u velocity component and skirt height y_{gap}.

2.3. GRID SIZE AND NUMBER OF ITERATIONS:

Uniform grid spacing is used in the calculation procedure, as indicated in figure (2). Twelve nodes are employed in both the horizontal and vertical directions (NI = NJ = 12). The height of the skirt gap y_{gap} is specified through the index JGAP, the height

is being (Y(JGAP)+Y(JGAP+1))/2, as shown in figure (2). JGAP takes the values 2, 4 and 6 in order to obtain the the various skirt heights employed in this study which are 0.1, 0.3 and 0.5 of the total height. The width of the roof slot of the support structure x_{gap} was specified form the index IGAP, the width equals to (X(IGAP)+X(IGAP+1))/2. IGAP is kept constant and equals to 4 that corresponds to 1.5 m wide.

Changing the grid size to 22 nodes in both the horizontal and vertical directions (NI = NJ = 22), does not affect the accuracy of the solution.

Ten iterations were employed in this investigation. After eight iterations only, a converging solution was obtained.

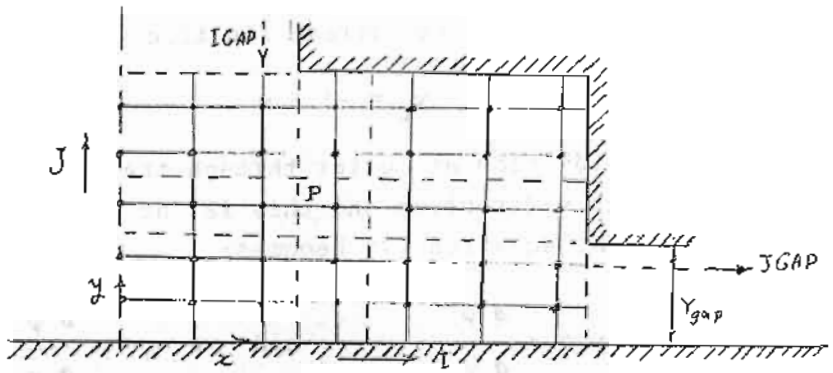

Figure (2) The numerical mesh employed in the calculations

3.CALCULATION ALGORITHM:

An algebraic, finite-difference counterpart of the differential equation (8) is derived for the representative cluster of grid nodes shown in figure (2). The procedure was made as follows: firstly equation (8) was integrated, as far as formal calculus allows, over the control volume surrounding P and simultaneously averaged over a finite increment of time δt; then the remaining integrals will be replaced by algebraic approximations [11]. This transfers the partial differential equation (pde) (8) into an algebraic equation.

Such equation can be written for each interior cell,

yielding a set of simultaneous algebraic equations, whose number equals to the number of unknown stream functions. The aim now is to solve these simultaneous equations.

In that program, a combination of iteration by lines and block adjustments is used. The aim is to achieve computational efficiency without excessive complication and computer storage.

The line iteration procedure involves simultaneous solution for the stream functions along each grid line, while the stream functions along neighboring lines are temporarily taken as known stream functions. The simultaneous solution is achieved by a particular form of Gaussian elimination known as "Thomas Algorithm" [12], or "tri-Diagonal Matrix Algorithm" (TDMA). This procedure is applied along north-south grid lines, starting at the westmost one and sweeping eastwards.

The action of the line iterative procedure is to sweep the errors in the prevailing solution of the stream function field to the boundaries, were they are reduced or eliminated by the boundary conditions. The errors are not reduced to zero in just one iteration. That is revealed by consideration of the residual sources R_p of the finite-difference equations [13].

The R_p's for the cells must ideally be zero, if the prevailing stream function field were without errors which can be achieved by the application of the TDMA to a grid line.

Unfortunately there are some circumstances in which the rate of reduction of the R_p's by the line-iteration procedure becomes unacceptably slow, This may happened when the resistance to the mass flow rate at the boundaries is large. Since it is the changes in boundary mass flow which effectively remove the errors, the effect of high resistance is to cause them to be reflected back into the interior field; without significant reduction.

An effective solution for this problem is to use a procedure which, by simultaneously adjusting the stream functions on each line by uniform increments for each line (the value of the increment varying from line to another) causes the R_p's to sum to zero along every line, and hence over the entire field. This procedure is known as the block adjustment procedure, the details of the procedure is clear in [14].

3.1. SOLUTION PROCEDURE:

The solution procedure starts from the initial distribution of the stream function ψ at time $t = t_o$. The initial distribution consists of the boundary condition values setted according to the mass flow rate and other node values which are assumed to be zero. Then the procedure advances to the next time level $t = t_o + \delta t$. For steady state condition, such as the case in question, only just one time step with δt effectively set equal to infinity can be performed. The procedure first evaluates the coefficients of the partial differential equations (pde) basing them on the prevailing stream functions as an initial estimate. Then, the stream functions are updated by first performing a line-iteration sweep and then making the block adjustments. The result so obtained is examined for satisfactoriness, by checking if the residual-source sum R_p is sufficiently small. If it is unsatisfactory, the cycle is repeated from coefficients calculation stage, until an acceptable solution is obtained. This provides the stream function field.

In practice, the quantities of interest are the velocity components u and v, and the pressure field p. Arrangements are therefore made in the program to calculate these quantities once a converged solution has been obtained for the stream function. Having the stream function ψ, finite difference versions of equation (7) are used in the program to calculate the values of u and v. Then, equation (10) was applied to obtain the values of the pressure field p, imposing the condition that ρ_t is uniform over the flow field.

4. RESULTS AND DISCUSSION:

Calculations are performed for the case of uniform inlet and outlet velocities. Firstly, three cases are investigated varying the skirt gap y_{gap} from $0.1h$ to $0.3h$ to $0.5h$, while the mass flow rate is kept constant. The inlet velocity v was kept constant at 0.667 m/s that corresponds to a stream function $\psi = 1.0$, equation (12), at both the top wall and right-hand side wall of the solution domain. The corresponding outlet velocities u for these

cases are 10 m/s, 3.33 m/s and 2 m/s respectively, according to equation (13) and the continuity equation. The stream lines (ψ = constant) are plotted in figures (3 to 5). These figures show that the stream lines become more denise as they approach the exit of the air cushion. The flow pattern looks like that one obtained from the flow of a real fluid around a corner. Figure (6) shows the variation of the average pressure, P, along the underside of the hovercraft floor, top wall of the solution domain, and the skirt height Y_{gap}. It indicates that the mean pressure, P, decreases as the skirt height increases. This is also expected because Bernoulli's equation (10) states that the total pressure P_t is uniform over the flow field and as the skirt height Y_{gap} is reduced the exit velocity u increases to maintain the flow rate constant, that makes the total pressure at the solution domain increases as well.

In figures (7 to 9), the skirt height Y_{gap} was kept constant at 0.3 of the total height H, while the inlet velocity υ increases. Three inlet velocities are employed in these cases namely 1.33 m/s, 2 m/s and 2.67 m/s that corresponds to mass flow rates (per unit length of the solution domain) $\dot{M}$ = 2 kg/s, 3 kg/s and 4 kg/s respectively. The flow pattern show no significant change in the general shape except that the value of of each stream line has in new value according to the total mass flow rate. The mean pressure along the underside of the hovercraft floor and the mass flow rate for constant skirt gap Y_{gap} = 0.3 H is plotted in figure (10). It indicates that the increase in the mass flow rate corresponds to an increase in the average pressure. The relation between them is a straight line when it is plotted in log-log axis, as shown in the figure (10). This behavior is expected for a real fluid flow since Bernoulli's equation is governing the relation between the pressure and the inlet velocity and, consequently, it controls the relation between pressure and the mass flow rate.

Further runs are made, for some largest gaps Y_{gap} = 0.2 H, 0.3 H, 0.4 H and 0.5 H; in which the inlet velocity was adjusted until the average pressure along the underside of the hovercraft floor is approximately the same as that pressure (P = 34.7 kp/cm^2)

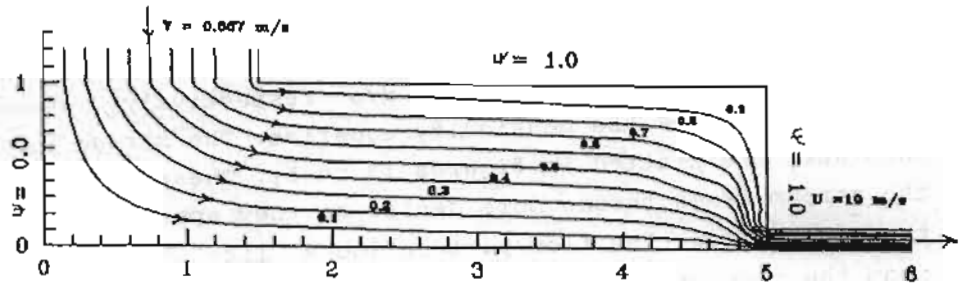

Figure (3) Stream lines for Y_{sep} = 0.1 H.

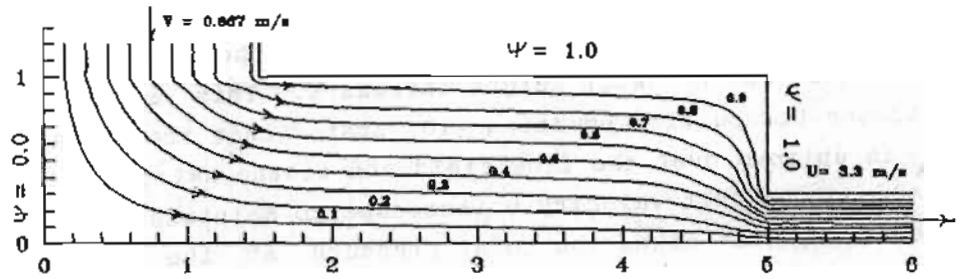

Figure (4) Stream lines for Y_{sep} = 0.3 H.

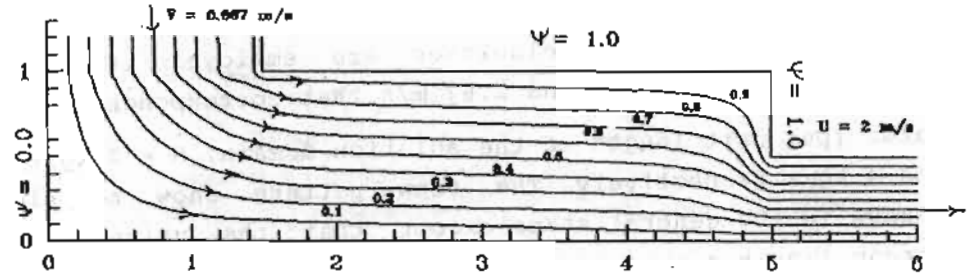

Figure (5) Stream lines for Y_{sep} = 0.5 H.

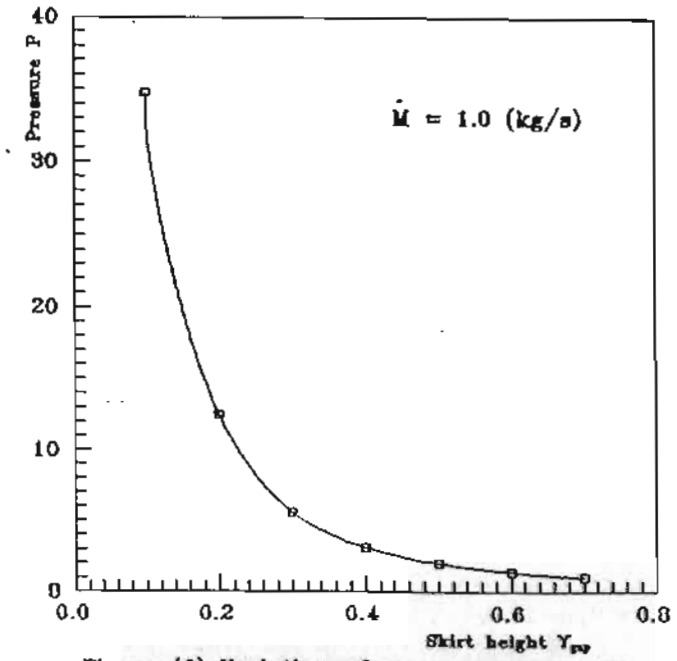

Figure (6) Variation of mean pressure with skirt height for constant mass flow rate.

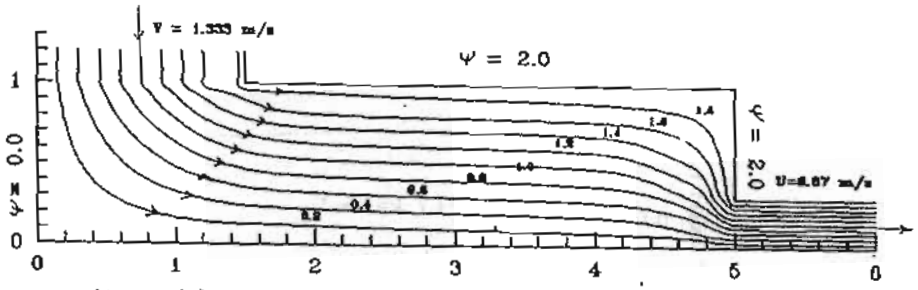

Figure (7) Stream lines for mass flow rate $\dot{M}$ = 2.0

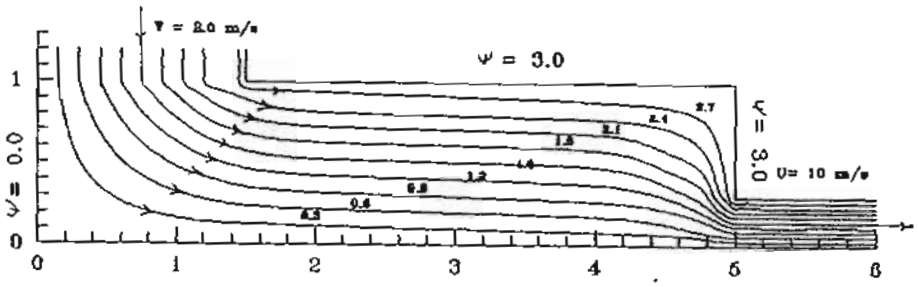

Figure (8) Stream lines for mass flow rate $\dot{M}$ = 3.0

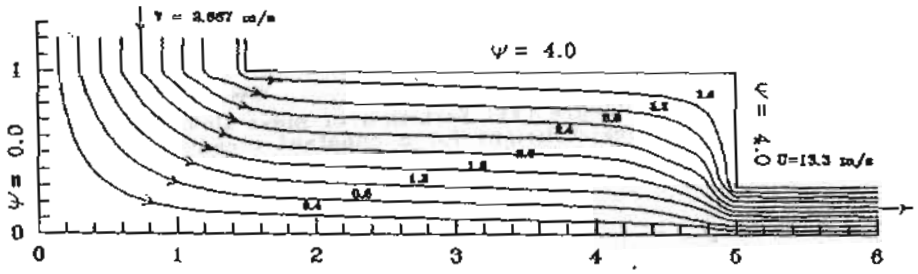

Figure (9) Stream lines for mass flow rate $\dot{M}$ = 4.0

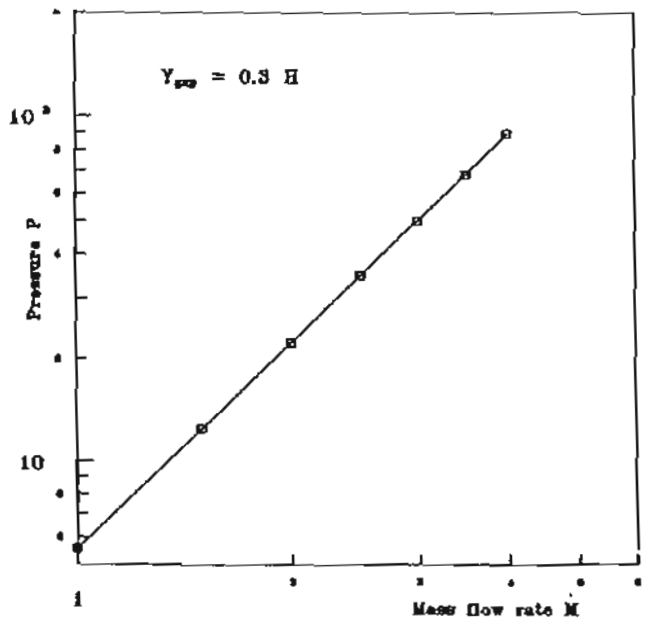

Figure (10) Variation of mass flow rate with mean pressure for constant skirt hight Y_{gap} = 0.3 H.

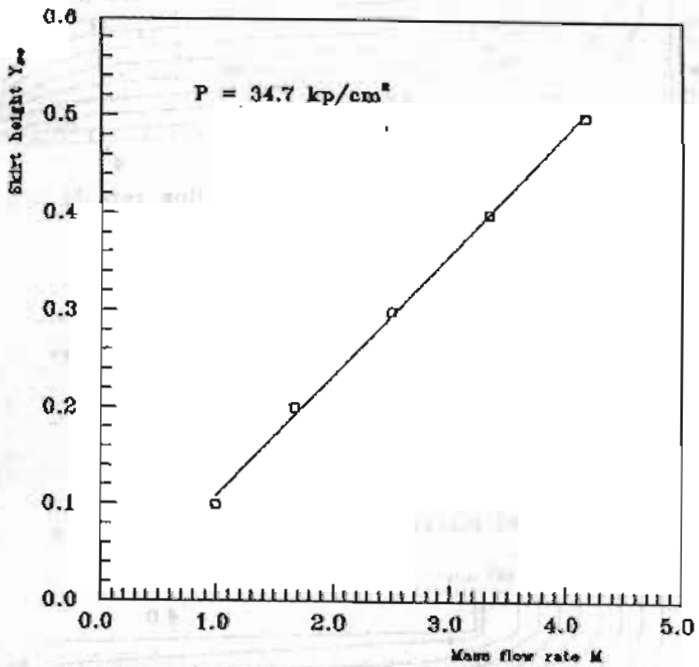

Figure (11) Variation of mass flow rate with skirt height for a constant mean pressure.

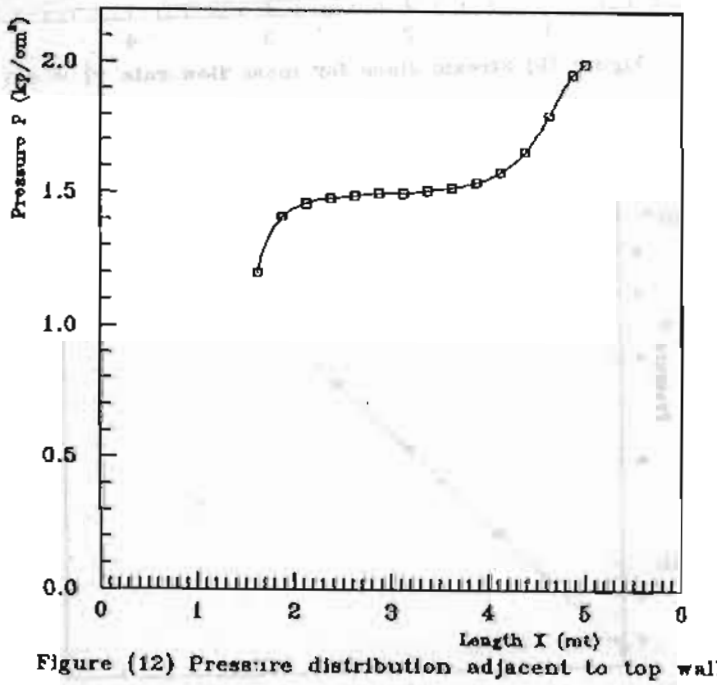

Figure (12) Pressure distribution adjacent to top wall

obtained form the smallest skirt height (0.1 H). The relation between the mass flow rate and skirt height for that constant pressure is represented in figure (11). It shows that relation is a straight line that means as the skirt height increases the mass flow rate must increase to maintain the mean pressure underside the hovercraft floor constant.

The pressure distribution adjacent to the top wall is represented in figure (12). The pressure has it minimum value at the nodes which are adjacent to the entrance where the inlet velocity has its maximum value then the pressure increases gradually until it reaches its maximum value at the right-hand corner where the velocity is almost zero.

This study may explain the practical limitation of the use of a hovercraft with the roughness of the ground or the water over which the craft must travel. The more rough is the surface, the larger in average, will be the gap under the hovercraft skirts Y_{gap}. As a result, the amount of air (M) required to "cushion" the craft is greater. There is of course a limit to the air supply that the craft's turbines can provide. Therefore, the craft (for example) is unable to operate over very rough seas.

5-CONCLUSIONS:

The employment of the irrotational flow model in investigating the flow pattern under a stationary hovercraft, at a constant mass flow rate, reveals that the flow pattern changes with the change of the relative height of the shirt (Y_{gap}/H), specially near the exit of the flow. While there is no change in the flow pattern with the increase of the mass flow rate if the skirt height is kept constant. The study of the mean pressure along the underside of the hovercraft floor indicated that the pressure decreases with the increase of the of the skirt height, if mass flow rate is maintained constant. For constant skirt height, the pressure increases with the increase of the mass flow rate. The variation of the mass flow rate with the skirt height, while keeping the average pressure along the underside of the hovercraft constant at a certain value, show that the mass flow rate increases linearly with the skirt height. All these parameters can be employed to

develop a relation between the power of the hovercraft turbines (required to deliver a certain mass flow rate) and the roughness of the ground or water over which the hovercraft will travel.

6. NOMENCLATURE:

C_v	Constant-volume specific heat capacity.
H	Height of the solution domain.
IGAP	Index for slot in the roof of hovercraft.
JGAP	Index for height of the skirt gap.
k	Thermal conductivity.
$\dot{M}$	Mass flow rate.
p	Static pressure.
p_t	Total pressure.
r	Radial coordinate in a cylindrical-polar frame.
S	Energy source.
t	Time.
T	Temperature.
δt	Time increment.
u	Longitudinal velocity component.
v	Tangential velocity component.
W	Width of the solution domain.
x	Longitudinal cartesian coordinate.
X_{gap}	Half-width of the slot in the roof.
y	Tangential cartesian coordinate.
Y_{gap}	Skirt gap height.
ψ	Stream function.
ω	Vorticity of the fluid.
ρ	Density.

7. REFERENCES:

1. Cutt, P.J., "Potential for the Air Cushion Vehicle in the Offshore Industry", Offshore and Arctic Operations, Petroleum Division (Publication) PD v 38, publ by ASME, New York, NY, USA, Jan. 1991, P 75-79.

2. Hinchey, M.J. and Sullivan, P.A., "On Hovercraft overwater heave stability", Journal of Sound and Vibration, V. 163 N. 2, May

1993, P 261-273.

3. Hinchey, M.J. and Sullivan, P.A., "Experiments on hovercraft overwater stability", 11th International Conference on Port and Ocean Engineering Under Arctic Conditions, POAC v 2, Can., Sep. 1991, P 939-952.

4.Sullivan, P.A. & Walsh, C. and Hinchey, M.J., "Kelvvin-Helmholtz Wave Generation Beneath Hovercraft Skirts", Journal of Sound and Vibration, V. 163 N. 2, May 1993, P 275-282.

5. Osuka, k. & Hayashi, R. and Ono, T., "Heave Dynamics Control of the Hovercraft via H Infinity Control Theory", Procc 92 Jpn USA Symp Flexible Autom., Publ by ASME, New York, NY, USA, Jul 1992,P 533-538.

6. Abulnaga, B.E., "Introduction to the Dynamics of Air Propelled Vehicles for Sand Deserts", Aeronautical Journal, V. 92 N. 918, Oct. 1988, P 328-335.

7. Eroshin, V.A. & Konstantinov, G.A. & Romanonkov, N.I. and Yakimov, Yu. L., "Experimental Determination of the Pressure on a Disk Entering a Compressible Fluid at an Angle to the Free Surface", Fluid Dynamics, Sep. 1988, P 174-178.

8. Schlichting, H. "Boundary layer theory", McGraw Hill, New York, 1968.

9. Massey, B.S., "Mechanics of fluid", Van Nostrand Reinhold, London, U.K., 1979.

10. Gosman, A.D.,"The TEACH-C Program for Calculating Heat Conduction", Mechanical Engineering Dept., Imperial College, Report CAL-C1-76, London, U. K., 1976.

11. Varga, R.S., "Matrix Iterative Analysis", Prentice-Hall, 1962.

12. Westlak, J.R., "A Handbook of Numerical Matrix Inversion and Solution of Linear Equations", John Wilew, 1968.

13. Roache, R.J., "Computational Fluid Dynamics", Hermosa Publishers, Albuquerque, 1972.

14. Patankar, S.V., "Numerical Heat Transfer and Fluid Flow", McGraw-Hill, 1980.